CARITAS UNIVERSITY AMORJI-NIKE, EMENE, ENUGU STATE
Caritas Journal of Engineering Technology
CJET, Volume 5, Issue 1 (2026)
Article History: Received: 21st Dec., 2025 Revised: 18th January, 2026 Accepted: 23rd January, 2026

Fluid Loss Control Materials From Hevea Brasiliensis and Egg Husks: A Comparative Study With MICA in Water-Based Mud

Daniel Erobo AKPOTU[1]
Ebikapaye Peretomode[1]
Iwemah Ejiro RUFUS[2]
Wilfred OKOLOGUME[3]
[1]Department of Petroleum Engineering, Delta State University, Abraka, Nigeria.
[2]Department of Civil Engineering, Delta State University, Abraka, Nigeria.
[3]Department of Petroleum Engineering, Federal University of Petroleum Resources, Effurun, Nigeria.
*Corresponding author: peretomodejeffery7@gmail.com

Abstract
The increasing demand for oil and gas has led exploration companies to adopt extensive drilling practices across diverse geological formations to access target reservoirs. These formations frequently pose challenges because they readily allow drilling mud infiltration, leading to substantial fluid losses during circulation. To address this challenge, the present study developed specialized fluid loss control materials derived from processed Hevea brasiliensis (rubber seed shell) and egg husks according to the API procedure. These materials were subjected to drying, grinding, and sieving to obtain two particle sizes (150 microns and 250 microns), which were then blended in equal proportions as alternatives to Mica, a conventional fluid-loss additive. Water-based mud samples incorporating these locally sourced additives were prepared at various concentrations and evaluated against Mica for performance. The results demonstrated that mixtures containing 3 wt.% (10.50 g) of 150 µm and 4 wt.% (14.00 g) of 250 µm particles exhibited fluid loss characteristics comparable to those of 2 wt.% Mica. Analysis of rubber seed shell revealed a complex mixture of organic compounds, with calcium identified as a major element in both materials. The local additives also enhanced the yield point and reduced gel values, thereby promoting more efficient cutting removal and improved penetration rates. Additionally, muds formulated with local additives exhibited increased pH, attributed to their high calcium content. These findings highlight the potential of locally sourced husk materials as effective fluid loss additives for drilling in loss-prone formations, providing a viable approach to mitigate downhole losses.

Keyword: fluid loss; husk materials; Hevea brasiliensis seed; water-based mud; cuttings removal; downhole losses.

1.0 Introduction

Exploration and production businesses must deploy technologies to tap deep-seated reservoirs as the world's energy demand continues to climb and hydrocarbon production declines daily. As a result, technology must be used more effectively to navigate various formations (Rana, et al., 2019). Arising from the fact that hydrocarbons are found deeper in subterranean formations, different formation types are drilled through; therefore, in order to successfully drill different geological formations containing diverse types of rocks, a drilling mud containing various chemical additives must be circulated. This is due to the fact that all well-drilled formations are diverse and lack homogeneity (Talukdar & Gogoi, 2015). The primary reason for the success of drilling operations is the properties of the mud. In addition to considering the mud rheology and filtration characteristics, drilling fluids must have sufficient viscosity to control fluid loss into the formation and to suspend the rock cuttings when drilling operations are halted (Oseh, et al., 2023). A vital function of drilling fluid is that it helps to gradually form a permeable filter cake around the wall of the borehole, which helps to

keep the bore stable pending the run-in-hole (RIH) of casing pipes. This further helps to control fluid loss into the formation (Oseh, et al., 2023; Odion, 2019). Filtration is the process of separating a liquid-solid system through a porous medium, whereby a part of the solid component is retained on the surface of the porous medium. Factors affecting filtration properties include concentration, thermal stability, dosage, size, types of solids, and contaminants inherent in the mud. Depending on the frequency and local history of a stuck pipe, modest values for fluid loss and filter cake can be established for a particular lithology (Ali, et al., 2022).

Fluid loss control additives produced from husk materials have been actively explored in successive years. For instance, rice husks have been investigated by many as a fluid loss reducer in water-based mud (WBM) (Okon, et al., 2020; Agwu, et al., 2019). Ash from rice husk was prepared and utilized as an additive in WBM to improve mud properties. At high concentrations of 15-20%, the local additive revealed improved fluid loss and filter cake thickness and also supports effective wellbore cleaning parameters such as yield point, gels and thixotropic property (Raza, et al., 2023). Similarly, the efficacy of an eco-friendly rice husk ash in WBM was investigated, at lesser than or equal to 15 weight percentage of this prepared additive into the spud mud, there were tremendous improvement in vital WBM properties such as reduced plastic viscosity being a signal that it supports the reduction of solids in the mud, improved mud thixotropy, yield point, apparent viscosity, drilled cuttings carrying capacity and fluid behavior index (Yalman, et al., 2021).

A polymer based WBM prepared with rice husk without the addition of bentonite and barite, it was reported that the presence of rice husk revealed improved excellent rheological and filtration property of the mud, it was also found that this special mud was prepared as a reservoir drill-in fluid possessing shale stability by inhibiting shale swelling and thus supports wellbore stability (Mech, et al., 2020). The potential of rice husk and corn husk as a possible eco-friendly additive in WBM was investigated in comparison with Carboxy Methyl Cellulose (CMC). The synergy of both materials with consistent particle size supports the various properties of drilling fluids and specifically maintains viscosity, fluid loss and also supports fluid stability. Cellulose derived from groundnut husk at different particle sizes was investigated at different concentrations. These cost-effective and environmentally friendly husks derived from groundnut were found to limit the volume of clear filtrates from the mud, thereby averting interaction with nearby formations, improving rheological properties (improved yield point and gel strength) with an increase in mud pH (Patidar, et al., 2020; Cheng & Heidari, 2017; Wang, et al., 2018).

Authors (Eze & Chukwu, 2025; Jimmy, et al., 2024; Nwala, 2024; Okon, et al., 2020; Idress & Hasan, 2020; AZUBIKE, et al., 2019; Amanullah, et al., 2016) have reported the use of dried sugar cane husk, dried palm kernel fiber, dried tiger nut husk, rice husk, sunflower seed, orange peel, date seed, corn hub, walnut shell, cassava starch, as loss circulation materials. However, these materials have different physicochemical properties. Hence, there is a need to further explore materials to reduce fluid loss while drilling ahead at elevated pump rates, and at the same time, possess the ability to improve rheology and other vital mud properties. This work seeks to further explore the use of husk material derived from *Hevea Brasiliense's* and egg as a more reliable additive to use in water-based mud.

2.0 Materials and methods

The materials used in this work include bentonitic clay, water, and *Hevea Brasiliense's* seed husk. Egg husk, barite, mica (fine), caustic soda, and soda ash.
The following equipment and set of apparatus were used during this study;
FTIR Spectrophotometer - FTIR 8400 S: This was used to determine functional groups and bond type associated with rubber seed shell and egg husks local materials. SEM-EDS: Used to ascertain the morphology and elemental composition of both local materials. Weighing scale: For measuring the desired weights of materials during mud formulation.
Blender: This is used for blending bentonite, water, and other additives.
Mud Balance: Mud balance was used to measure the density of mud.
API fluid loss tester: A low-pressure low low-temperature (LPLT) filter press machine was used to ascertain the rate of fluid loss (clear filtrate) and the thickness of mud cake from the whole mud.

pH meter: The pH meter measured the degree of concentration of hydrogen ions in the mud.
Marsh funnel viscometer: This was used to determine the quick viscosity of the mud. It measures how long (seconds) for a quart of mud will flow through the orifice of the marsh funnel.
Fann Rheometer (Rotational viscometer): This was used to determine the full rheological properties of the mud samples.

2.1 Preparation of Hevea Brasiliense's Seed Husk and Egg Husk

The *Hevea Brasiliense's* seed husk (Figure 1b & 1d) and egg husks (Figure 1a & 1c) purchased from the Oleh market, Delta state, Nigeria, as seen in Figure 1, were sun dried for 8 days until no moisture was found in them. They were ground by a warring blender repeatedly until they became fine particles. The grating process was repeated until the husk material was smooth to the touch by hand. Two mesh sizes of 150 micron and 250 microns were used to sieve both materials so as to obtain separate particle sizes. The important of this work is that both materials were grafted together as a single fluid loss additive, that is, 150 microns of *Hevea Brasiliense's* seed husk was grafted with 150-micron egg husk; this was tagged as local material a (LMat A). This was also done for the 250-micron materials and tagged as local material b (LMat B).

Figure 1: (a) egg husks (b) Hevea Brasiliense seed husk (c) grafted egg husk (d) grafted Hevea Brasiliense seed husk

2.2 Determination of Physicochemical Properties of Local Materials

2.2.1 Fourier Transform Infrared test (FTIR)

The Shimadzu Fourier transform Infrared Spectrophotometer—FTIR 8400 Sas was used to determine functional units. Samples were weighed at 0.01 g by a mortar and agate and homogenized with 0.01 g KBr anhydrous. The mixes were vacuum hydraulically pressed at 1.2 Pa to produce transparent pellets. The tested sample's spectrum was reported after the scanned sample passed through the infrared spectrum and was recognized by a detector attached to a computer as a continuous wave. Typically, samples were scanned in the 600 to 4000 cm^{-1} absorbance range. As the foundation of the spectrum type Spectrophotometer, the analysis's findings include the chemical structure, molecular binding form, and specific functional groups of the tested substance. A UV spectrophotometer made by PG Instruments, model T70, was used to evaluate the sample at various wavelengths. Prior to doing the calibration using distilled water and a black body, the spectrophotometer's absorption was turned on to allow for stabilization. After calibration, the wavelength was set to 330 nm, and after pushing the key for absorption, the corresponding absorption was shown. Up until 900 nm, this technique was repeated for various wavelengths.

The samples that had already been electrically grounded were correctly labeled into their corresponding stubs and dried at 60 ºC. A vent switch was used to pressurize the chamber holding the sample with nitrogen at a pressure of 50 Pa. When the holder stub with the sample and vacuum pressure of $5x10^{-5}$ Pa was integrated, the instrument's door was shut. The filament height and the monitor, which turned on automatically, both released a potential differential of 15 KV. A solid-state tool used in an energy-based detector that separates X-ray energy and properly analyzes X-ray emissions depending on the number of atoms produced by the electron beam. When the holder stub with the sample and vacuum pressure of $5x10^{-5}$ Pa was integrated, the instrument's door was shut. By allocating the proper elements to the sample, the chemistry of the atoms on the specimen's surface is ascertained.

2.3 Drilling Fluid Preparation

They were done sequentially with the mud composition as shown in Table 1. 350 ml of water was measured into an industrial blender, and 25 pounds per barrel (33.25 g) of bentonite was weighed and added into the water already in the blender under constant stirring for 10 minutes. This concentration is to ensure that the expected marsh funnel viscosity will be high enough to suspend all other chemical additives in the WBM formulation. The mixture was kept idle for 8 hours to allow bentonite to yield. The yielded spud mud was then subjected to agitation, and other mud chemicals, as presented in table 1, were added one after the other. The first mud sample prepared was without an LCM material which is referred to as NFLA, sample B and C contained 1 wt.% and 2 wt.% of Mica (F) respectively, sample C, D, E, F and G contained 1 wt.%, 1.5 wt.%, 2 wt.%, 3 wt.% and 4wt.% respectively of the local material containing 150 micron blend, sample H, I, J, K and L was prepared with 1 wt.%, 1.5 wt.%, 2 wt.%, 3 wt.% and 4 wt.% respectively of a 250 micron sized blend of the new material under study. A blend of the local material was compared to the properties of Mica (Fine), an industrial grade material selected as a lost circulation material being used in the drilling industry. The weight percentages of the lost circulation materials were based on the weight of the base fluid (water) being used to prepare the mud samples. The density of water used in preparing the mud samples was initially checked and was 1 gram per milliliter, this means, the weight of 1 milliliter of water is 1 gram, and therefore, 350ml of water used in preparing each mud sample is 350 g.

Table 1: Mud composition

Mud sample	*Water (ml)*	*Soda Ash (g)*	*Caustic soda (g)*	*Bentonite (g)*	*Barite (g)*	*Xanthan Gum (g)*	*Mica (F) (g)*	*L Mat (A) (g)*	*L Mat (B) (g)*
NFLA	350	4	4	33.25	3	1	-	-	-
A	350	4	4	33.25	3	1	3.50	-	-
B	350	4	4	33.25	3	1	7.00	-	-
C	350	4	4	33.25	3	1	-	3.50	-
D	350	4	4	33.25	3	1	-	5.25	-
E	350	4	4	33.25	3	1	-	7.00	-
F	350	4	4	33.25	3	1	-	10.50	-
G	350	4	4	33.25	3	1	-	14.00	-
H	350	4	4	33.25	3	1	-	-	3.50
I	350	4	4	33.25	3	1	-	-	5.25
J	350	4	4	33.25	3	1	-	-	7.00
K	350	4	4	33.25	3	1	-	-	10.50
L	350	4	4	33.25	3	1	-	-	14.00

2.4 Drilling Fluid Testing

2.4.1 Filtration Property Test

The API fluid lost test is a low pressure, room-temperature piece of equipment for mimicking the property of WBM at downhole conditions of the top-hole section of wells being drilled. The instrument is made up of a main frame, base cap, mud cell and top cap containing a vent valve, a port receptacle for pressuring the

instrument. The base cap contains a rubber gasket, a 200-mesh screen, and a filter paper. The mud cell was locked into the properly dressed base cap, and the mud sample meant for investigation is transferred into it to half an inch from the top. The sample was then placed on the main frame, and the top cap was placed on the mud cell. The T-screw on top of the main frame was used to secure the mud cell by continuously turning it clockwise while ensuring that the vent valve was in the closed position. The vent valve was closed before turning on the CO_2 cartridge at its port. The adjustable T-screw on the top of the top cap was continuously being closed so as to provide pressure into the sample already inside the mud cell. Immediately, the pressure gauge records 100Pa pressure, and the release of pressure into the mud cell was stopped. A 25 ml-sized measuring cylinder was placed under the mud cell so as to collect clear filtrate from the mud after 30 minutes; this is referred to as fluid loss volume. The instrument was carefully dismantled, and the cake deposited on top of the filter paper was measured in millimeters by a Fann ruler.

2.4.2 Rheological property *of mud sample*
The detailed rheological property of the mud sample was determined by the Fann rheometer. The agitated mud sample was poured into the mud line on the mud cell and then placed under the rotor sleeve. The rotor sleeve was precisely immersed to the scribed line in order to acquire various revolution per minutes (rpm) of 600 rpm, 300 rpm, 200 rpm, 100 rpm, 6 rpm, and 3 rpm.
The instrument's left leg's lock screw was tightened to maintain this position. The crank was turned for roughly 15 seconds while the gear shift was in the high-speed position. Then, it was released to turn the crank to 600 rpm and kept turning. For further rheometer speed settings of 300 rpm, 200 rpm, 100 rpm, 6 rpm, and 3 rpm, were repeated.

2.4.3 Mud Density
The Ofite mud balance is made up of a case used in carrying the mud balance itself. The carrying case of the mud balance was opened via the locks fitted at both ends. The carrying case contained a knife edge upon which the fulcrum of the mud balance was carefully made to sit. The lid of the mud cell was opened, and the freshly prepared mud was poured into it to the brim. The mud cell lid was placed back, and the excess mud or any trapped air in the mud was seen to spill out through its tiny hole (vent). The exterior part of the mud cell, upon the excess spilled mud stained was properly wiped off with a rag. The rider which possesses the ability to balance the weight of the content inside the mud cell was moved left and right such that the spirit level inside the level glass was seen at its midpoint. The value of the rider, which coincides with the calibrated rider arm, was recoded as the density of the mud in pounds per gallon (ppg) or any other unit of choice.

2.4.4 Mud pH
The PHS-25 PH meter contains a pH probe and temperature probe, was standardized by preparing buffer solutions of pH 6.86 and 10.1. This was done by diluting a pill of each pH stated above in 1000 mL of water separately. Transfer each of these buffer solutions into two beakers, one for rinsing the electrode, while the second is for calibrating the instrument. The pH electrode was dipped into the buffer, and the screw corresponding to the pH value under calibration is adjusted until value displayed correspond to the pH of the buffer solution. This was done for both pH values stated above. The instrument is now ready for use to determine the pH value of the mud samples. In order to determine the pH value of the mud sample, the sample was given a little stir, and the pH was observed until the pH meter readings stabilizes. Report temperature and pH values between 0 and 14. The electrode was cleaned in water, and then the protective electrode cap was replaced.

2.4.5. Marsh funnel viscosity (MFV)
The marsh funnel used is composed of a 6-inch cone, a 12-inch height, a 2-inch tube, and a 10-mesh size that covers half of the cone. While holding the instrument upright, the prepared mud is passed through the mesh to remove any solid material that could block the funnel aperture. A thumb was used to cover the tip of the tube, making sure that the mud contacted beneath the mesh. A quart of mud is the amount of mud sample that is poured into the marsh funnel (equal to 946 ml), a stopwatch was used to record the moment the entire amount of mud flowed through the aperture and out of the marsh funnel.

3.0 Results and Discussion

3.1 Determination of functional group and bond type of local materials using Fourier Transform Infrared (FT-IR)

The elements, compounds, bond types, and functional groups present in *Hevea Brasiliense's* seed husk and egg husk are illustrated by the FT-IR spectrum in Figure 2. The FTIR spectra of the rubber seed shell show several absorption bands corresponding to different functional groups. The broad band around 3024.90 cm^{-1} indicates O-H stretching vibrations, which may be due to hydroxyl groups or adsorbed water molecules (Zhang, et al., 2021; Stumm, 1997). Bands at 2918.79 cm^{-1} and 2162.89 cm^{-1} are characteristic of C-H stretching, indicating the presence of alkanes or aliphatic compounds (Kumar, et al., 2023; Moreira, et al., 2017; Manh-Thuong, et al., 2013). Bands at 1600.14 cm^{-1} and 1491.96 cm^{-1} can be attributed to C=C stretching, indicating the presence of aromatic rings or alkenes. The band at 1451.11 cm^{-1} may result from C-H bending in alkanes or aliphatic compounds. Bands at 1373.69 cm^{-1} and 1067.82 cm^{-1} are assigned to C-O stretching vibrations, suggesting the presence of alcohols, ethers, or esters. Absorption bands at 1027.15 cm^{-1}, 905.32 cm-1, 748.20 cm^{-1}, and 694.78 cm^{-1} are due to out-of-plane C-H bending in aromatic compounds (Baitimbetova, et al., 2022). The band at 535.84 cm^{-1} may correspond to C-S stretching, indicating the presence of sulfur-containing compounds. These identified functional groups suggest that the rubber seed shell contains a complex mixture of organic compounds, such as aliphatic and aromatic compounds, alcohols, ethers, esters, and sulfur-containing substance.

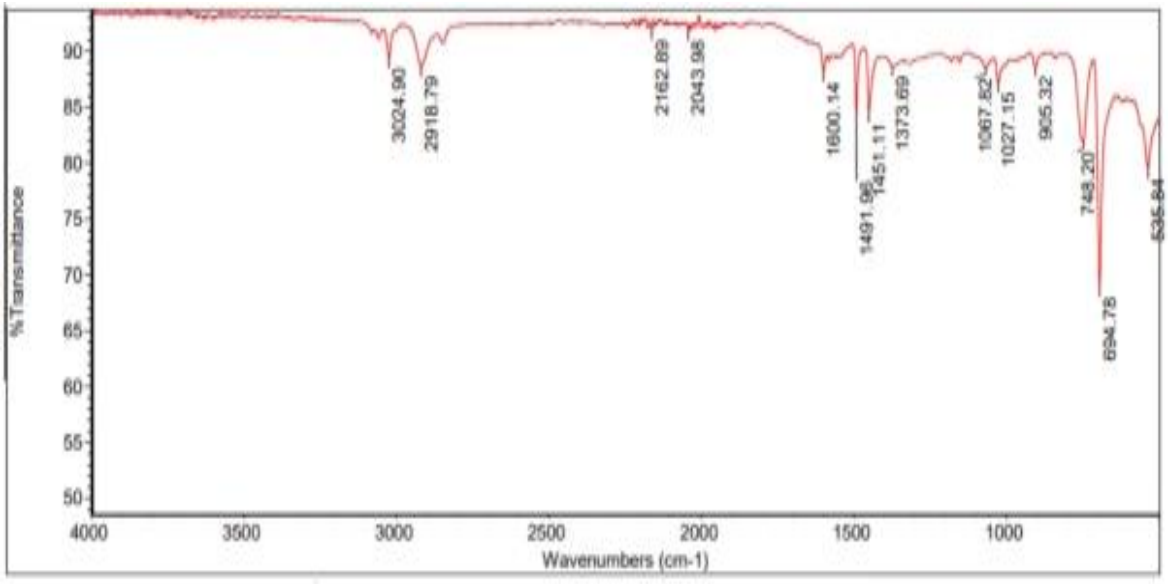

Figure 2: FTIR Spectra of Rubber seed shells

3.2 FTIR Spectrum for Pulverized Egg Shell

The Fourier-Transform Infrared (FTIR) spectrum of grounded egg shell is presented in Figure 3. As revealed in the FTIR spectrum of the ground Egg shell presented in Figure 9, the sample has several distinct absorption peaks. The key absorption peaks observed in the spectrum are located at 537.80 cm^{-1}, 695.45 cm^{-1}, 754.69 cm^{-1}, 906.10 cm^{-1}, 1027.68 cm^{-1}, 1373.17 cm^{-1}, 1451.48 cm^{-1}, 1492.09 cm^{-1}, 1600.47 cm^{-1}, 2921.04 cm^{-1}, and 3024.59 cm^{-1}. The peaks around 1400-1600 cm^{-1} correspond to C=C and C=O stretching vibrations, indicating the presence of aromatic and carbonyl groups (Cheng, et al., 2022). These groups could be associated with organic compounds present in the eggshell matrix. The peaks in the 2900-3000 cm^{-1} range suggest the presence of C-H stretching vibrations from alkane groups (Sari, et al., 2023). These aliphatic hydrocarbon groups are commonly found in organic materials. The lower wavenumber peaks below 1000 cm^{-1} can be attributed to various bending and rocking vibrations of the mineral components (Kumar, et al., 2023) in the eggshell, such as calcium

carbonate. Egg shells are primarily composed of calcium carbonate, which is a key structural component. The presence of these functional groups suggests that the ground eggshell sample is a complex material composed of both organic and inorganic components. The organic compounds may include proteins, lipids, and other biomolecules, while the inorganic component is likely dominated by the calcium carbonate mineral.

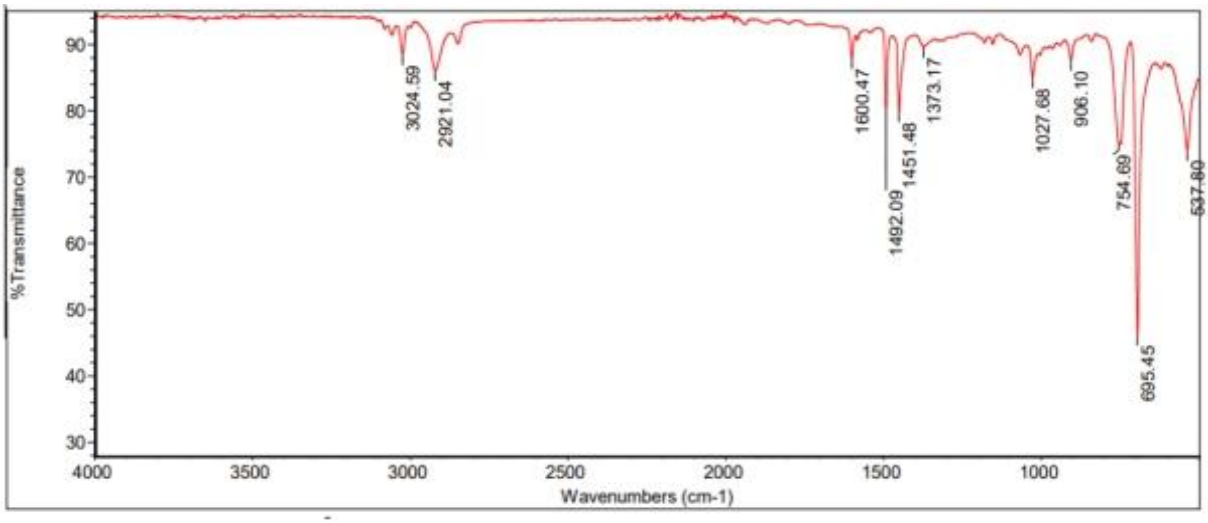

Figure 3: FTIR Spectrum of grinded Egg shells

3.3 Determination of morphology, elemental composition using scanning electron microscopy and energy dispersive X-ray spectroscopy (SEM-EDS)

Figure 4a, 4b, and Figure 5a and 5b revealed the SEM-EDS of *Hevea brasiliensis* seed husk and egg husk, respectively. This is a non-destructive approach, and can be used to examine the structure and elements that make up both materials. Egg husk contains mainly calcium (92.09%), Yttrium (1.6%), silver (1.52%), with traces of potassium, niobium, iron, chlorine, sulfur, titanium, silicon, aluminium, magnesium, carbon, sodium, and phosphorus. Also, *Hevea brasiliensis* seed husk contains, silicon (45.95%), calcium (34.71%) as dominant materials with iron (3.89%), titanium (3.87%), potassium (3.25%), yttrium (2.54%) and silver (2.06%) with other trace elements as niobium, chlorine, aluminium, sulfur, magnesium, sodium, and phosphorus. Calcium, being the dominant material in both materials, has applications in cement manufacture, plastics, and adhesives, which are materials that can aid in sealing formation walls to reduce loss of mud into the formation.

Figure 4a: SEM image at 200 µm

Table 2: Elemental distributions in Hevea brasiliensis seed husk

Element Number	Element Symbol	Element Name	Atomic Conc.	Wt. Conc.
20	Ca	Calcium	93.37	92.09
39	Y	Yttrium	0.73	1.60
47	Ag	Silver	0.57	1.52
19	K	K	1.00	0.96
41	Nb	Nb	0.34	0.78
26	Fe	Iron	0.41	0.56
17	Cl	Cl	0.62	0.54
16	S	Sulfur	0.53	0.42
22	Ti	Ti	0.32	0.37
14	Si	Silicon	0.46	0.32
13	Al	Al	0.41	0.27
12	Mg	Mg	0.32	0.19
6	C	Carbon	0.60	0.18
11	Na	Sodium	0.23	0.13
15	P	P	0.07	0.05

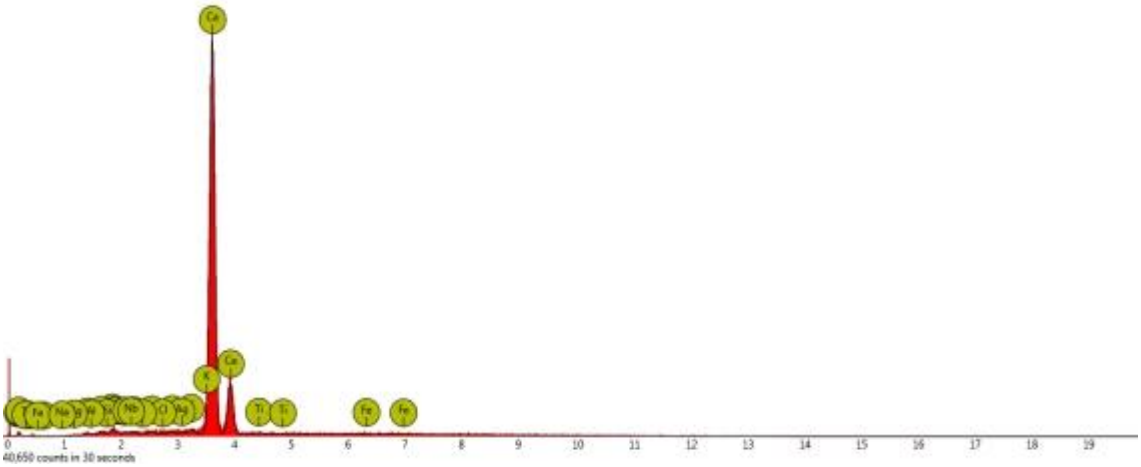

Figure 4b: EDS of Hevea brasiliensis seed husk

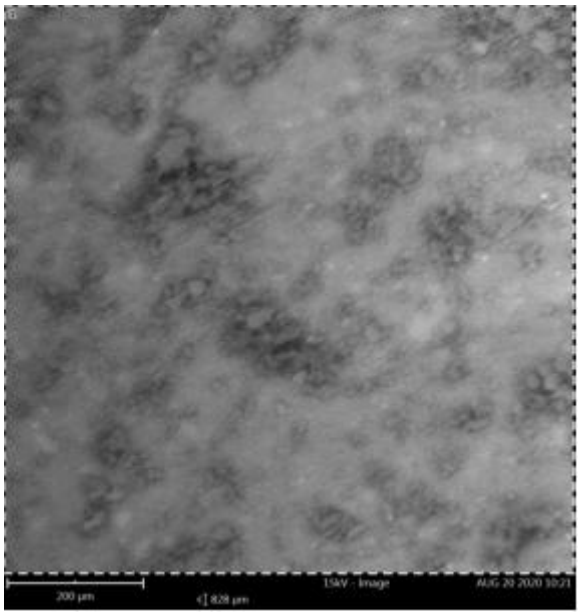

Table 5a: SEM image at 200 µm

Table 3: Elemental Distribution in Egg Husk

Element Number	Element Symbol	Element Name	Atomic Conc.	Weight Conc.
14	Si	Silicon	49.55	45.95
20	Ca	Calcium	38.96	34.71
26	Fe	Iron	2.11	3.89
22	Ti	Titanium	2.45	3.87
19	K	Potassium	2.52	3.25
39	Y	Yttrium	0.87	2.54
47	Ag	Silver	0.58	2.06
41	Nb	Niobium	0.32	0.99
17	Cl	Chlorine	0.61	0.71
13	Al	Aluminium	0.52	0.69
16	S	Sulfur	0.56	0.60
12	Mg	Magnesium	0.55	0.44
11	Na	Sodium	0.41	0.31
15	P	Phosphorus	0.00	0.00

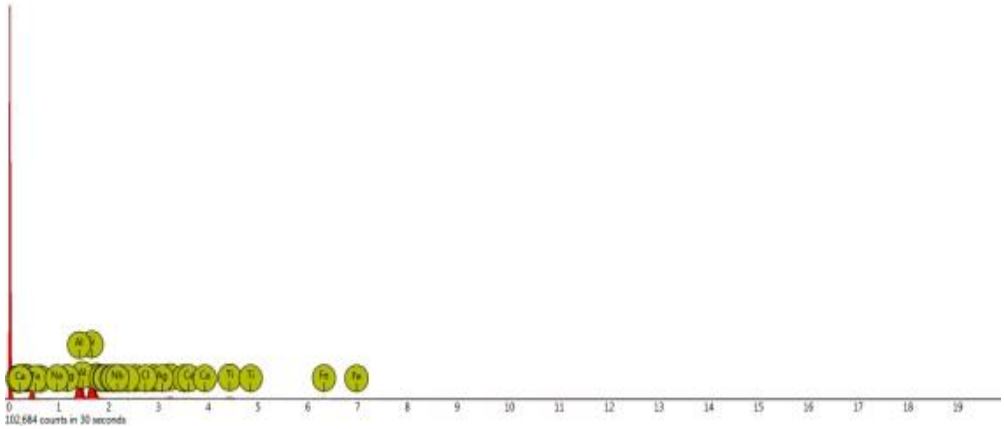

Figure 5b: EDS of Egg husk

3.4 Filtration property

Figure 6 presents the filtration property results of all the water-based muds, fluid loss (FL), and cake thickness (CT). The volume of clear filtrate (ml) and cake thickness (mm) is seen to be high in the mud sample without a fluid loss additive (NFLA). From the results, fluid loss reduced from 15 ml to 1.8 ml, while cake thickness reduced from 3.2 mm to 2.3 mm for samples A and B comprising mica being an industrial fluid loss control additive. It can be seen from the plot that an increase in concentration of the fluid loss additive led to an improved filtration property. The locally grafted materials at 3 wt.% (10.50g) of 150µm and 4 wt.% (14.00g) of 250µm, possess similar fluid loss performance as 2 wt.% of mica. This means that the local additive can be adopted as a fluid loss additive in water-based mud, though at a double concentration. The performance is similar to other husk materials reported by Agwu et al. (Agwu, et al., 2019), where rice husks were utilized with enhanced fluid loss and filter cake thickness. At high concentration, the locally grafted material provided an excellent spurt loss than the mica additive.

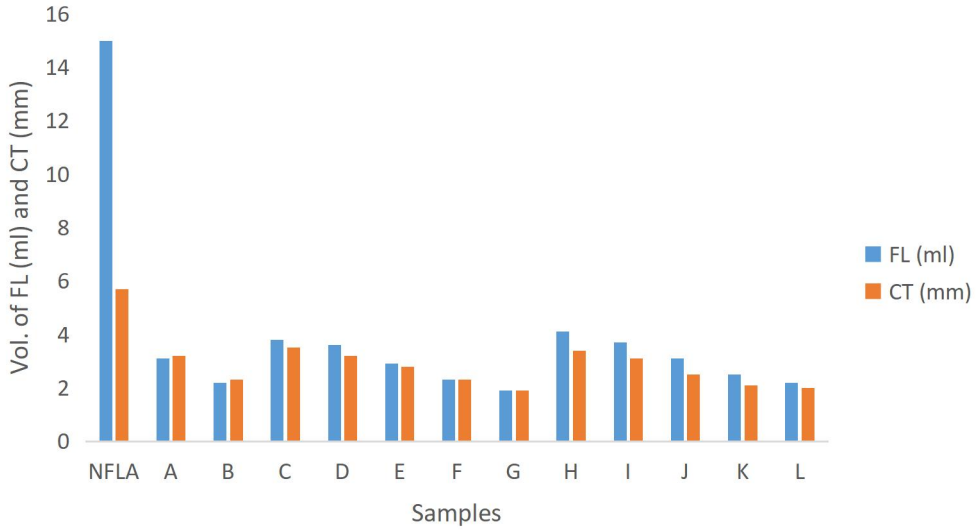

Figure 6: Filtration property of various drilling fluids

3.5. Plastic viscosity and Yield point

The rheological property often referred to as the viscosity of drilling fluid was evaluated using a standard rheometer operated at room temperature. The rate of shear of the drillings generated viscosity values reported in centipoise, and two types of viscosity values were calculated: plastic viscosity (PV), yield point (YP). Plastic viscosity and yield point of various mud samples are presented in Figure 7. From the results, all plastic viscosities were greater than 20 cp. However, the introduction of mica and locally blended fluid loss additives further increased the plastic viscosity in all water-based mud samples. The plastic viscosity of all the samples increased as the concentration of fluid loss additives increased. This increase was a result of solids concentration, solids size, and shape, arising from the fluid loss additives. The yield point of the water-based drilling fluids was also calculated from the data generated from the viscometer reading. From the result, it can be seen that YP of the drilling fluids reduced with an increase in the concentration of mica and the locally prepared fluid loss additives. However, it can be seen that the addition of the local additive at a lower concentration exhibits a relatively higher yield point than the mud without a fluid loss additive. This is contrary to Azubuike et al. (2019) who reported an increase in the yield point using rice husk.

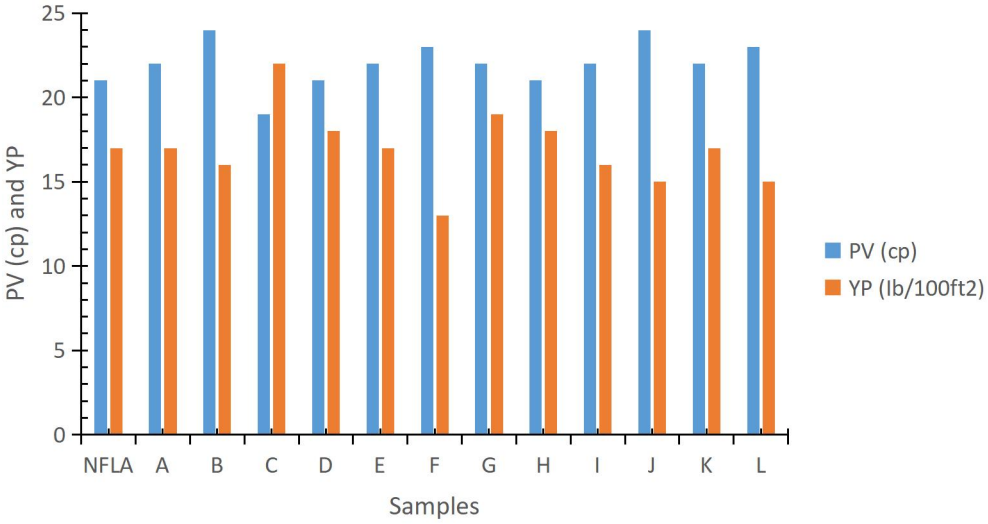

Figure 7: Plastic viscosity and Yield point of drilling fluid systems in this work

3.6. Gel strength

The gel strength of the various water-based mud was measured to understand how the new fluid loss additive derived from husk materials influenced the water-based mud at a time when the muds were halted. From the results presented in Figure 8a, the industrial-grade material (mica) did not influence the gel values; this is because the bland mud has a similar gel nature to that of mica-blended mud. Meanwhile, low concentrations of 150-micron local materials possessed similar gels as the industrial grade, as both presented a 5 lb/100 ft² difference between initial and final gel values. But higher concentrations of 250-micron local additive tend to possess a progressive gel nature due to the 7 lb/100 ft² - 8 lb/100 ft² difference between initial and final gel strengths. This behavior could be due to larger particle sizes and higher concentrations of the locally grafted materials. Therefore, it is crucial to carefully consider the particle sizes and concentration when selecting them as a fluid loss additive.

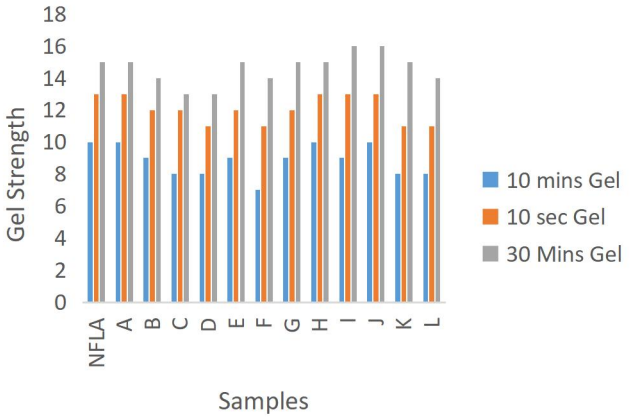

Figure 8a: Gel strength at 10sec and 10mins

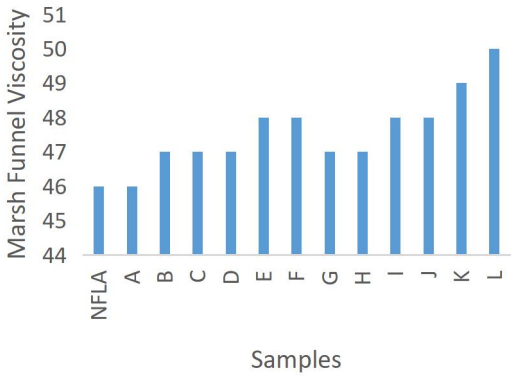

Figure 8b: Marsh Funnel Viscosity for mud samples

The flow behavior of the various fluid loss additives developed from mica and locally made husk materials used in water-based mud is presented in Figure 8b. From the results, the use of mica at a low concentration does not have a significant effect on the marsh funnel viscosity of the drilling fluid. But an increased concentration of mica resulted in an increased marsh funnel viscosity. But the use of local materials increased the funnel viscosity of the mud. At a higher concentration and larger particle sizes, the funnel viscosity values increased further.

3.7. Mud Weight

The weight of the mud, determined by using a standard mud balance, was investigated so as to ascertain how the locally sourced husk materials would contribute to the hydrostatic pressure of the mud. From the results presented in Figure 9, it can be seen that fluid loss additives tend to reduce overall mud weight across all the mud samples. The higher the concentration of the fluid loss additives, the lower the mud weight. This may be due to the formation of foam in the mud (Ali, et al., 2022). Again, it was also observed that the effect of the fluid loss additive reducing the mud weight was more in the finer particle sizes than in the larger particle sizes. However, the mud weight reported in all the mud samples containing LCM made from mica (F), 150 micron and 250 microns of the new material are within range of mud weight for drilling top hole across the globe (8.6 ppg to 9.3 ppg). In operations where there is need to increase mud weight, chemical additives such as barite or calcium carbonate could be mixed into the mud to maintain weight so as to main hydrostatic pressure to prevent influx of formation fluid into the wellbore.

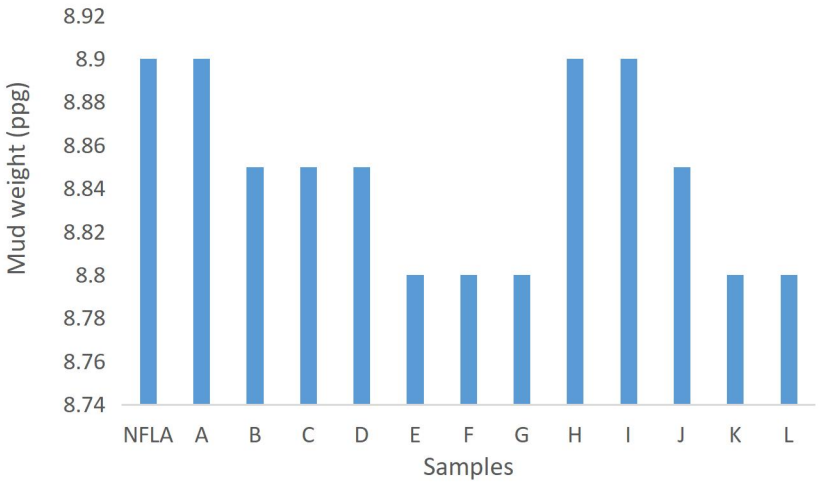

Figure 9: Mud weight against mud samples

3.8. Mud pH

The effect of the fluid loss additive on the mud pH is presented in Figure 10. The mud samples prepared using the foreign additive had a very low effect on the pH of the mud samples. Whereas, the local additive supports the degree of the concentration of hydrogen ions in the mud samples prepared by the local fluid loss additives. At a high concentration, the pH of the various mud samples tends to increase; it was further revealed that the higher the concentration of the local materials, the greater the increase in the mud pH values across all the mud samples. The increase in the pH of the mud samples is attributed to the presence of calcium at high atomic concentration combines with lower concentrations of sodium and potassium in the local material as shown by the EDS and the presence of hydroxyl in the shown by FTIR (Zhang, et al., 2021). The presence of the above chemical compositions signifies the materials influence the pH of the mud positively. This is a vital property of a WBM which helps not only to main PH of the mud but also helps to fight the effect of bacteria's especially when the spud WBM is left unused for days thereby helping to main the rheology of the mud (Long, et al., 2016; Yamamoto, et al., 2010). Also, with this performance, drilling professionals could reduce the concentration of caustic soda used in preparing the bentonite mud in the presence of this new material as a lost circulation material of choice.

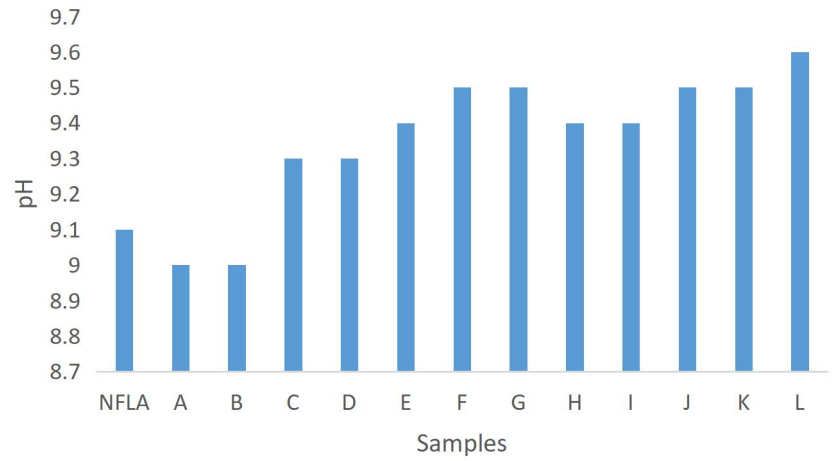

Figure 10: Mud pH against mud samples

4.0 Conclusion

The volume of mud lost during drilling of the top-hole formation using WBM is a huge challenge and calls for urgent attention to reduce the amount of chemicals spent in drilling this section of the oil and gas well. A local additive made from Brasiliense seed husk and egg husk grafted together was deployed as a possible replacement for use as a fluid loss additive; the performance of the local materials was compared to Mica (Fine), an industrial-grade fluid loss control additive. The combined husk materials contain mainly calcium, silicon, and aluminum, as revealed by SEM-EDS. The presence of hydroxyl groups in the blended materials, reflected by the FTIR, and the abundance of silicate and potassium in both materials from SEM-EDS, is a testament that these local LCM additives are similar to all forms of mica, such as muscovite, phlogopite, biotite, and lepidolite. Calcium, being a contributor of binding materials used in cement production, could be responsible for creating a barrier on the filter cake to prevent loss of mud into the formation. The locally grafted materials were excellent as fluid loss additives in water-based mud at relatively higher concentrations. Both particle sizes provided quality filtration properties, but the lower particle size was more effective as a fluid loss additive. This is due to the reduction in the pore spaces by the lower size particles which led to a reduction in the rate at which mud is permeated into the formation. The plastic viscosity, yield point, and initial and final gel of all the drilling fluid samples had relatively similar values. The local additive, when used at increasing concentrations, was found to enhance the pH of the drilling fluids across all levels of concentration. This is vital and very key since water-based mud pH is expected to be alkaline. The best filtration property was realized by 14 g, which represents 4 wt.% of 150 microns of grafted local additive.

Conflict of Interest: The authors declare no conflict of interest

References

Agwu, O., Akpabio, J. & Archibong, G. (2019). Rice husk and saw dust as filter loss control agents for water-based muds. *Heliyon,* p. 5(7)..

Ali, I., Ahmad, M. & Ganat, T. (2022). Experimental study on water-based mud: investigate rheological and filtration properties using cupressus cones powder.. *J Petrol Explor Prod Technol 1,* 2(https://doi.org/10.1007/s13202-022-01471-8), p. 2699–2709 .

Amanullah, M., Ramasamy, J., Al-Arfaj, M. K. & Aramco, S. (2016). Application of an indigenous eco-friendly raw material as fluid loss additive.. *Journal of Petroleum Science and Engineering,* 139(https://doi.org/10.1016/j.petrol.2015.12.023), pp. 191-197.

Azubuike, A., Yakubu, Y. & UGOCHUKWU, A. (2019). Evaluation of the Impacts of Locally Sourced Lost Circulation Materials on Drilling Muds Properties. *IRE Journals,* 2(2), pp. 2456-8880.

Baitimbetova, B. et al. (2022). The study of carbon nanomaterials by IR-Fourier spectroscopy, obtained by the action of an ultrasonic field on graphite.. *Bulletin of the Karaganda University. "Physics" Series. ,* pp. https://doi.org/10.31489/2022ph2/127-132..

Cheng, K. & Heidari, Z. (2017). Combined interpretation of NMR and TGA measurements to quantify the impact of relative humidity on hydration of clay minerals. *Appl. Clay Sci., ,* Volume 143 , pp. 362-371, 10.1016/j.clay.2017.04.006.

Cheng, X. et al. (2022). Vibrationally-Resolved X-ray Photoelectron Spectra of Six Polycyclic Aromatic Hydrocarbons from First-Principles Simulations. *The journal of physical chemistry. A,* p. https://doi.org/10.1021/acs.jpca.2c04426.

Eze, S. O. & Chukwu, C. J. (2025). Formulation of drilling fluids using local materials.. *European Journal of Sustainable Development Research,* 9(3. https://doi.org/10.29333/ejosdr/16352.), p. 308.

Idress, M. & Hasan, M. (2020). Investigation of different environmental-friendly waste materials as lost circulation additive in drilling fluids.. *J Petrol Explor Prod Technol ,* 10(https://doi.org/10.1007/s13202-019-00752-z.), p. 233–242 .

Jimmy, D. E., Benedict, U. W. & Igani, O. (2024). *Comparative Study of Loss Circulation Additives (Conventional and Local Materials) for Filtration Control..* Lagos, Nigeria, s.n.

Kumar, M. et al. (2023). Dielectric Response and Electric Modulus Studies of Polythiophene/Reduced Graphene Oxide Nanocomposites.. *Materials Science Forum, ,* pp. 1099, 69 - 74..

Long, X. et al. (2016). The effect of water molecules on the thiol collector interaction on the galena (PbS) and sphalerite (ZnS) surfaces: A DFT study. *Appl. Surf. Sci., ,* Volume 389, pp. 103-111, 10.1016/j.apsusc.2016.07.084.

Manh-Thuong, N., Seriani, N. & Gebauer, R. (2013). Water adsorption and dissociation on alpha-Fe2O3(0001): PBE+U calculations. *J. Chem. Phys., ,* Volume 138 , p. 10.1063/1.4804999.

Mech, D. et al. (2020). Formulation of a rice husk based non-damaging drilling fluid and its effect in shale formations.. *Energy and Climate Change,* pp. 1, 100007..

Moreira, G. et al. (2017). XPS study on the mechanism of starch-hematite surface chemical complexation. *Miner. Eng., ,* Volume 110 , pp. 96-103, 10.1016/j.mineng.2017.04.014.

Nwala, S. (2024). *"Tests On Locally Sourced Mud Bio-Additives Show Better Rheological and Loss Circulation Control Properties to Enhance Drilling Performance and Guarantee Energy Supply..* Lagos, s.n.

Odion, A. J. (2019). *Formulation of Water Based Drilling Fluid Using Local Mud Uwheru & Otor-Udu Clay..* Nigeria, OnePetro..

Okon, A. N., Akpabio, J. U. & Tugwell, K. W. (2020). Evaluating the locally sourced materials as fluid loss control additives in water-based drilling fluid.. *Heliyon,* p. 6(5).

Oseh, J. O. et al. (2023). Rheological and filtration control performance of water-based drilling muds at different temperatures and salt contaminants using surfactant-. *Geoenergy Science and Engineering,* pp. 228, 211994.

Patidar, A. K., Sharma, A. & Joshi, D. (2020). Formulation of cellulose using groundnut husk as an environment-friendly fluid loss retarder additive and rheological modifier comparable to PAC for WBM.. *Journal of Petroleum Exploration and Production Techn,* pp. 10(8), 3449-3466.

Rana, A., Arfaj, K. & Saleh, T. (2019). Advanced developments in shale inhibitors for oil production with low environmental footprints–A review.. *Fuel,* pp. 247, 237-249..

Raza, A. et al. (2023). Rice husk ash as a sustainable and economical alternative to chemical additives for enhanced rheology in drilling fluids.. *Environmental Science and Pollution Research,* pp. 30(48), 1056.

Sari, M. et al. (2023). Synthesis and Characterization of Activated Carbon/Alginate-Cu Composites. *Indonesian Journal of Chemical Science and Technology (IJCST),* p. https://doi.org/10.24114/ijcst.v6i2.49372..

Stumm, W. (1997). Reactivity at the mineral-water interface: dissolution and inhibition. *Colloids Surf. A: Physicochem. Eng. Aspects, ,* Volume 120 , pp. 143-166, 10.1016/S0927-7757(96)03866-6.

Talukdar, P. & Gogoi, S. B. (2015). Effective role of XC-polymer in the non-damaging drilling fluid (NDDF) for tipam sand of geleki oilfield of upper assam basin.. *International Journal of Research in Engineering and Applied Sciences,* pp. 5(5), 16-33..

Wang, X. et al. (2018). The adsorption mechanism of calcium ion on quartz (101) surface: A DFT study. *Powder Technol., ,* Volume 329 , pp. 158-166, 10.1016/j.powtec.2018.01.086.

Yalman, E., Depci, T., Federer-Kovacs, G. & Al-Khalaf, H. (2021). A new eco-friendly and low cost additive in water-based drilling fluids.. *Rudarsko-geološko-naftni zbornik,* pp. 36(5), 1-12..

Yamamoto, S. et al. (2010). Water Adsorption on alpha-Fe2O3(0001) at near Ambient Conditions. *J. Phys. Chem. C, ,* Volume 114, pp. 2256-2266, 10.1021/jp909876t.

Zhang, H. et al. (2021). Adsorption mechanism of water molecules on hematite (1 0 4) surface and the hydration microstructure.. *Applied Surface Science,* pp. 550, 149328.